Origin of the solid-state luminescence of MIL-53(Al) and its connection to the local crystalline structure

L. G. Barbata,[a] D. Scavuzzo, [a] R. Ettlinger,[b] M. M. Calvino,[a] G. Lazzara,[a] F.M. Gelardi,[a] S. Agnello,[a] M. Cannas,[a] Russell E. Morris,[b] and G. Buscarino[a]

a Dipartimento di Fisica e Chimica - Emilio Segrè, Università di Palermo, Via Archirafi, 36, I-90123 Palermo (Italy)

b EastChem School of Chemistry, University of St Andrews, North Haugh, St Andrews, UK

Corresponding author: gianpiero.buscarino@unipa.it

Abstract

Metal-organic frameworks (MOFs) are extensively studied due to their unique surface properties, enabling many intriguing applications. Breathing MOFs, a subclass of MOFs, have gained recent interest for their ability to undergo structural changes based on factors like temperature, pressure, adsorbed molecules. Certain MOFs also exhibit remarkable optical properties useful for applications such as sensors, light-emitting diodes, and scintillators. The most promising MOFs possess high porosity, breathing properties, and photoluminescence activities, allowing for improved device responsiveness and selectivity. Understanding the relationship between crystal structures and photoluminescence properties is crucial in these cases. As studies on this topic are still very limited, we report for the first time an exhaustive study on the solid-state luminescence of the breathing MOF MIL-53(Al), that can stabilize in three different crystalline structures: open-pore, hydrated narrow-pore and closed-pore. We unveil a fascinating solid-state luminescence spectrum, comprising three partially overlapping bands, and elucidate the intricate electronic transitions within each band as well as their intimate correlation with the local crystalline structures. Our characterizations of spectroscopic properties and decay times provide a deeper understanding of the luminescent behaviour of MIL-53(Al) and demonstrate that is possible to identify present crystalline structures by

optical measurements or to modify the optical properties inducing structural transitions for this type of materials. These insights could help to design next-generation, selective sensors or smart light emitting devices.

Keywords: MOFs, MIL-53, Breathing, Luminescence, Light emission

1. Introduction

Modern society is driven by the invention and use of more and more (increasingly complex) electronic devices. This revolution goes hand in hand with the increasing need of more efficient and specialized electronic components such as sensors, light-emitting diodes (LEDs), and scintillators. Having control over the optical response of a material, for instance by exploiting its structural behaviour, is a key challenge. Due to their hybrid nature, high degree of structural predictability and tunability, the crystalline porous material class of metal-organic frameworks (MOFs) is of particular interest for addressing this challenge in many fundamental applications, including sensors, displays, scintillators, imaging agents [1,2]. Consisting of metal ions or clusters and organic linkers [3,4], MOFs are highly versatile and modifiable and exhibit very intriguing properties, such high accessible surface areas, which makes them promising for many different applications like gas storage [5,6], adsorption and separation [7,8], catalysis [9,10], and drug delivery [11,12]. Among all the MOFs synthesized so far [13], the MIL-53 family (MIL=Matériaux de l′Institut Lavoisier) has gained notable interest for its fascinating physicochemical properties making it an example of prototypical MOF and one of the first MOFs commercially available [14,15]. These MOF structures are based on a trivalent metal ion (Al^{3+}, Cr^{3+}, Fe^{3+}…) linked by benzene-1,4-dicarboxylic acid (BDC or terephthalic acid). The most studied MIL-53 is the MIL-53(Al), involving Al ions [16,17]. A notable property of MIL-53 is the fact that they change structure upon external stimuli, as for example temperature [18,19], pressure

[20,21] or adsorption of specific molecules [22,23]. This property is termed as *breathing* [24]. MIL-53(Al), in particular, can assume three different structures: *i)* open pore (OP) with pore volume of 1432 Å and orthorhombic *Imma* crystalline structure, *ii)* hydrated narrow pore (HyNP) having pore volume of 949 Å and monoclinic *Cc* crystalline structure and *iii)* close pore (CP) structure having pore volume of 934 Å and monoclinic *C2/c* crystalline structure. The OP structure is usually obtained by thermal treatment at about 470 K in vacuum. A subsequent thermal treatment of the same sample at 77 K in vacuum stabilizes the CP structure. Since the phase transition between OP and CP structures as a function of temperature is hysteretic, the CP structure is preserved even when the sample temperature is subsequently raised from 77 K up to room temperature [25,26]. The HyNP structure is typically observed when MIL-53(Al) is in a strongly hydrated state [27,28,29].

Moreover, MIL-53(Al) exhibits remarkable photoluminescence observed under UV light excitation. Yang *et al*. [30] reported that MIL-53(Al) exhibits a strong luminescence band peaking at 425 nm with a lifetime of 5.6 ns upon excitation with light of wavelength 305 nm in an aqueous solution. The authors have attributed this luminescence to a ligand to metal charge transfer (LMCT) in which the photon is first absorbed by the BDC ligand, then the excited electron is transferred to the nearby metal ions, where it undergoes a radiative decay, generating the observed luminescence band.

An *et al*. [31] have studied the photophysical properties of MIL-53(Al) in powder form in air. They reported that upon excitation with light of 295 nm, a luminescence spectrum consisting of two partially superimposed bands is observed, with peaks at approximately 425 nm (2.9 eV) and 460 nm (2.7 eV). The band peaked at 425 nm was similar to that observed for powders of BDC in molecular form, peaked at 400 nm (3.1 eV), but with a red shift and a more complex time response. Based on these analogies, the band was attributed to a radiative decay taking place within the BDC ligands of the structure. Although experimental evidences have clearly indicated the existence of at least two distinct luminescence bands in the spectrum, no effort has been made to address the origin of the second contribution in the spectrum peaked at about 460 nm (2.7 eV).

The observation of two distinguishable bands in the spectrum of MIL-53(Al) is an important property that may indicate that different luminescence mechanisms are possible within one framework. Since the material exhibits breathing properties, it is also possible that the same luminescence mechanism produces bands with varying spectroscopic properties, depending on the particular crystal structure the material adopts locally around the site of radiative decay. It is surprising that in literature there are no studies on the possible correlation between breathing of MIL-53(Al), which is the forefather breathing MOF, and its luminescence while there are some examples for others breathing MOFs showing this correlation. For instance, Xiao *et al*. [32] have synthesized a Zn-based luminescent MOF showing a red shift of the peaks as a consequence of the structural breathing induced by adsorption of guest molecules, such as moisture or *N*,*N*-dimethylformamide. Yao *et al*. [33] developed an Eu-Tb co-doped MOF that exhibits a change of its characteristic luminescence from orange to green following a temperature induced structural breathing. Wang *et al*. [34] have reported a Cd-based breathing MOF that shows blue fluorescence, green excimer emission or orange room temperature phosphorescence depending on the structure it assumes. Therefore, it is evident that is possible to control the optical response of such materials by exploiting their structural breathing behaviour, making them very promising selective sensors or smart light emitting devices for example.

Here we present a comprehensive characterization of the luminescence properties of MIL-53(Al) in powder form, with the main focus of identifying all possible luminescence processes that take place in the material in order to unveil the existing connections between spectroscopic and time decay properties of the luminescence bands and the local structure assumed by the crystal. To obtain a complete characterization, the samples were characterized by powders X-Ray diffraction (PXRD), thermogravimetric analysis (TGA), scanning electron microscopy (SEM) and nitrogen sorption analysis.

2. Experimental

MIL-53(Al) used in this work is in powder form, of commercial origin and purchased by Sigma-Aldrich (Basolite® A100). Starting from this material two distinct samples of MIL-53(Al) were prepared. The first one was obtained by activating raw powders at 423 K in air in a glass tube overnight and then sealing it (denoted as **MIL-53(Al)**). The second one was prepared by dispersing raw powders in water and then left to dry at room temperature in air (denoted as **MIL-53(Al)-Hy**). A third sample was also considered, for comparison, consisting in a powder of terephthalic acid (denoted as **BDC**) in powder form purchased by Sigma-Aldrich.

Time-resolved luminescence (TRL) measurements were performed on samples in powder form contained in glass tubes by using an OPOTEK VIBRANT tuneable laser (pulse length of 5 ns, repetition rate 10 Hz) coupled with a Princeton Instruments Acton SP2300i spectrograph with PI-MAX CCD detector. All the TRL spectra were acquired at a fixed excitation wavelength of 305 nm (bandwidth=4nm), with a grating having λ_{blaze}=300 nm and 150 groves/mm, slit aperture of 1mm and spectral resolution of 20 nm. TRL spectra were recorder from 5 ns to 19 ns from laser pulse with a gate width of 1ns. The power of laser pulses used was kept at a constant value of 2μW.

PXRD measurements were performed in glass capillaries with a STOE STADI P machine in Debye-Scherrer mode using Mo Kα1 radiation. TGA measurements were performed with a TA Instruments - Q5000 IR apparatus in an inert atmosphere of nitrogen. Measurements were made from 25 °C to 800 °C and scanning rate of 20 °C/min.

SEM images were collected using a JEOL JSM-IT800 microscope. The powdered samples were placed on copper tape. BET-specific surface area determination from N_2 isotherms (77 K) was carried out according to the Rouquerol theory [35] using the Microactive Software Kit v4.03.04. Data was recorded on a Micromeritics Tristar II Surface Area and Porosity Instrument. The sample (~50 mg) was added to a frit tube and activated in vacuum (150 °C or 400 °C, ~3×10-5 mbar, 12 h) prior to the measurement.

3. Results

3.1. Material characterization

The crystalline structure of the samples MIL-53(Al) and MIL-53(Al)-Hy were studied by PXRD measurement, and the results are reported in Fig.1. The comparison of these data with those reported in literature, also reported in Fig.1 as vertical lines [21,23,36,37], indicates that MIL-53(Al) is mostly composed by OP structure, with minor contributions of CP and HyNP structures. At variance, in MIL-53(Al)-Hy both OP a HyNP structures are present in comparable proportions, whereas CP contribution remains marginal also in this sample.

The TGA obtained for pristine MIL-53(Al) powders indicates a first weight loss at about 100 °C and a further loss at about 500 °C, as shown in Figure S1, and is in good agreement with the results previously reported for commercial MIL-53(Al) [38]. The first characteristic temperature is related to the desorption of water molecules previously absorbed by the material, while the second is due to the irreversible decomposition of the crystal.

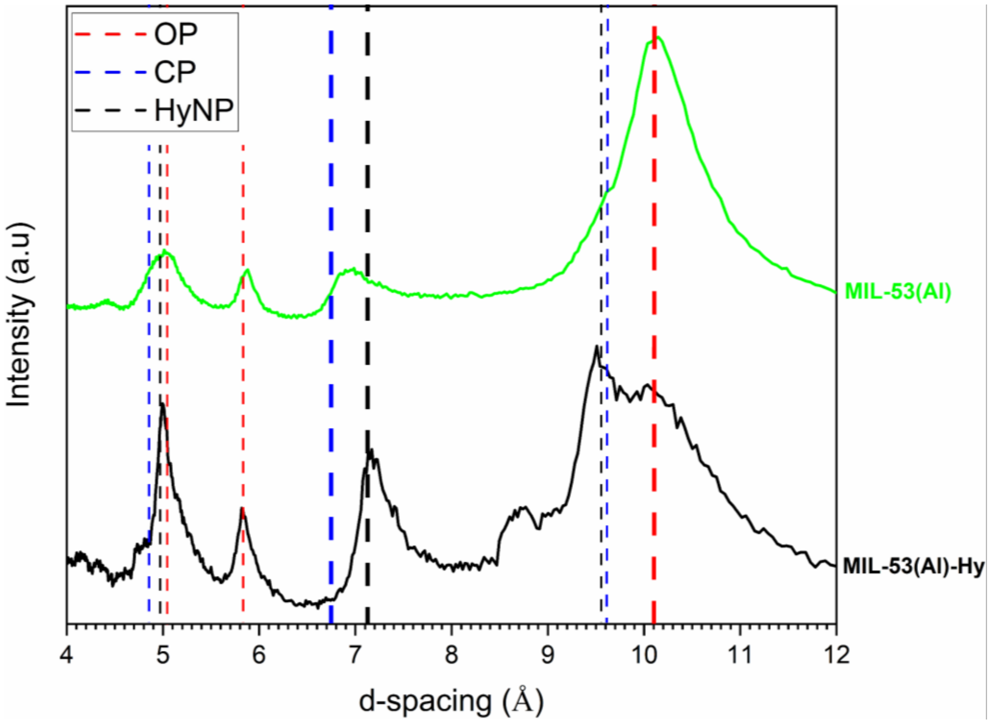

Fig.1: PXRD patterns of the samples MIL-53(Al) and MIL-53(Al)-Hy. Dashed lines represent the positions of the peaks pertaining to the three possible structures of MIL-53(Al), while their thickness is related to the expected corresponding peak intensity [4,21,34,35].

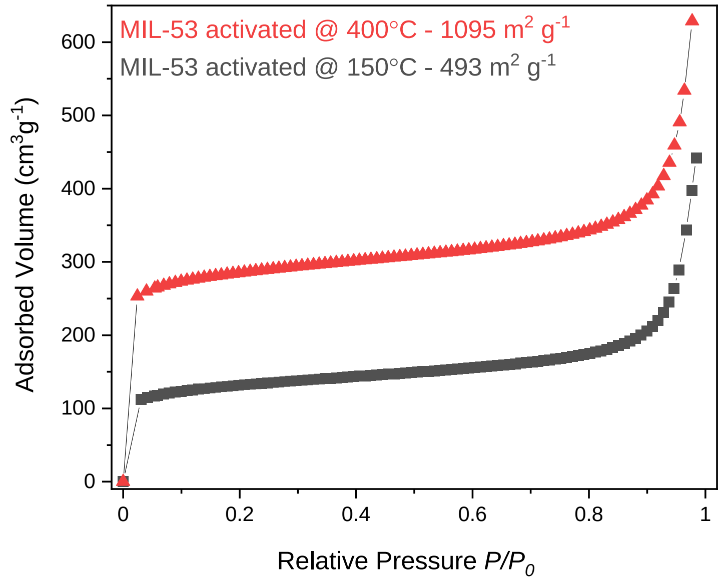

Fig.2: N_2 sorption isotherms (77 K) obtained for pristine MIL-53(Al) powders after activation at 150 °C or 400 °C.

Nitrogen sorption isotherm at 77 K were recorder for MIL-53(Al) activated at 150 °C or 400 °C (Fig.2). The recorded isotherms clearly show that an activation temperature of 150 °C is insufficient to remove strongly bound water and that only upon activation at 400 °C the BET surface area increased from 493 cm^2/g to 1095 m^2/g, that is in line with those previously reported for commercial MIL-53(Al) [39,40].

SEM analysis of the pristine MIL-53(Al) powders in Fig. 3 shows that the MOF features small needle-like particles that agglomerate into larger spheres with size of 7 ± 2 µm. Their broad particle size distribution between 100 to 850 nm and the significant variability in shapes cause the noticeable broadening of the PXRD reflections (Fig. 1). These results by the way are in accordance with those reported in previous works [41,42]. The preparation of MIL-53(Al)-Hy, which was obtained by dispersing MIL-53(Al) in water and drying at room temperature, did not alter the morphology of the material (Fig. 3b and d).

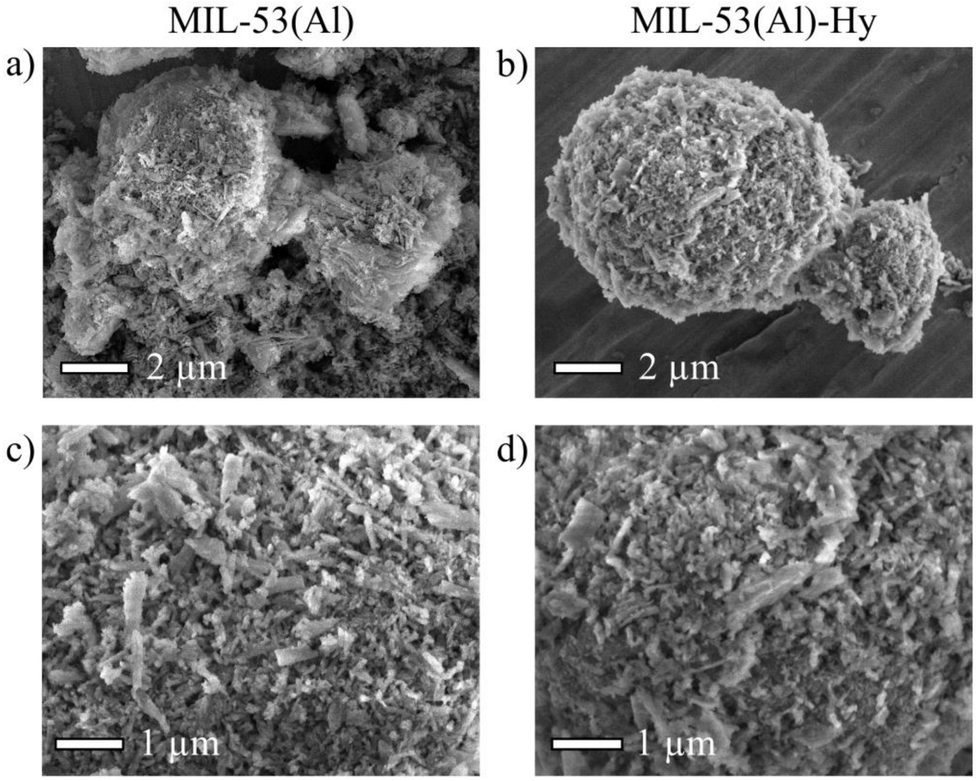

. Fig. 3: SEM images of MIL-53(Al) (a and c) MIL-53(Al)-Hy (b and d) particles; scale bar a-b) = 2 µm, and c-d) = 1 µm.

3.2. Optical properties of MIL-53(Al) and BDC

Analysing the optical properties, MIL-53(Al) showed laser sensitivity and its luminescence spectra underwent significant changes upon prolonged exposure to the laser (Fig. S2). To avoid laser-induced overheating of the sample, measurements were done using a significantly reduced power level of the excitation radiation by reducing the transmission efficiency of the laser beam. The studies performed have shown that the spectra acquired at the selected low power conditions, P = 2 μW, do not change as a result of prolonged exposure to the laser beam.

The solid-state luminescence spectra of MIL-53(Al), MIL-53(Al)-Hy and BDC were obtained by excitation at the fixed wavelength of 305 nm, which was found to maximize the amplitude of the luminescence spectra, in agreement with previous experimental reports [30,31]. The spectrum obtained for BDC after a time delay of 5 ns from the exciting laser pulse is reported in Fig. 4. It exhibits a single symmetric band peaked at 3.11 ± 0.05 eV (400 nm) and having full-width-at-half-maximum (FWHM) of about 0.63 ± 0.04 eV. Furthermore, the band undergoes a small red shift on increasing the time delay. This property is shown in Fig. S3, where the normalized spectra acquired for BDC after time delays of 5 ns and 19 ns are superimposed, showing a red shift of about 0.04 eV. The detailed study of the time response of the luminescence band observed for BDC is shown in Fig. 5, where the area of the band is reported as a function of the time delay from the exciting laser pulse. These results were fitted by assuming a single exponential decay, allowing to estimate a characteristic lifetime of τ_{BDC} = 5.5 ± 0.5 ns. The best fit curve is also shown in Fig. 5 superimposed to the experimental data, for comparison.

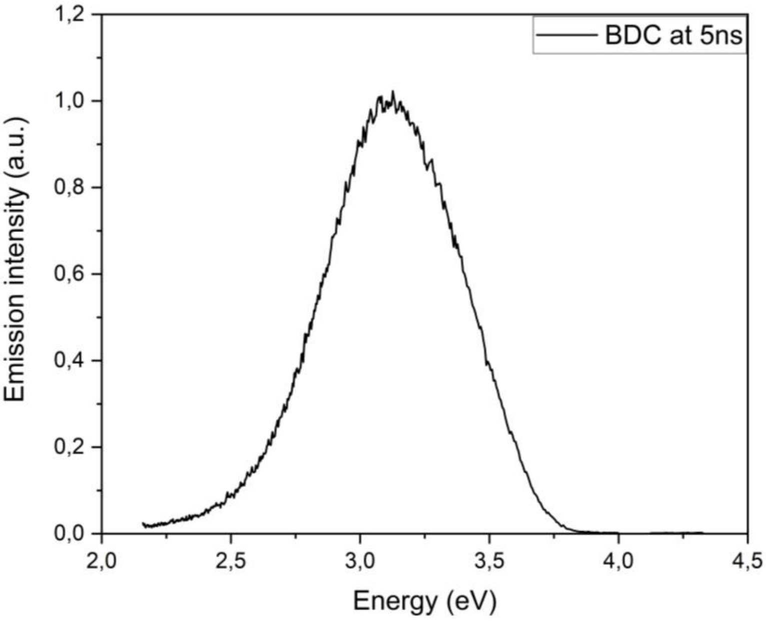

Fig. 4: Solid state luminescence spectrum obtained for BDC after a delay time of 5 ns from the exciting laser pulse.

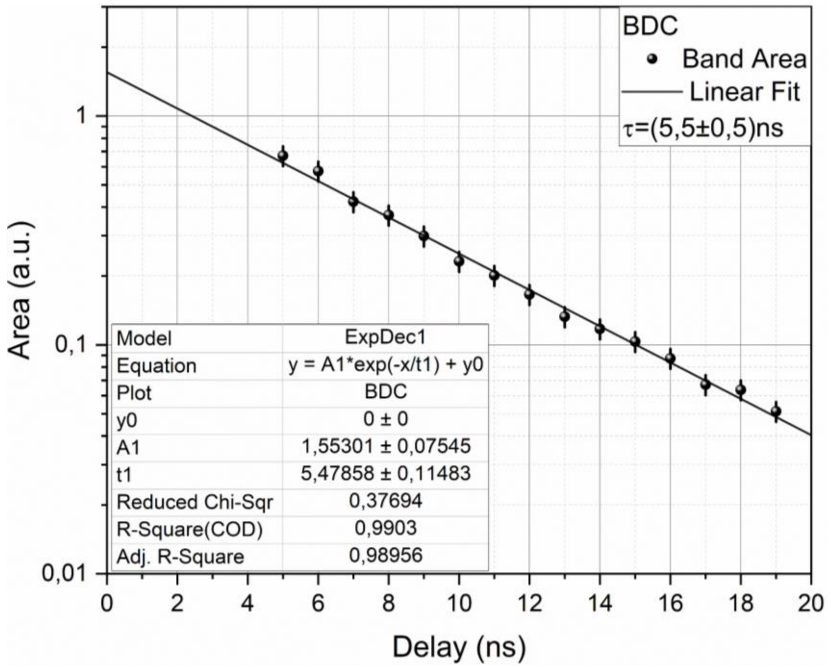

Model	ExpDec1
Equation	y = A1*exp(-x/t1) + y0
Plot	BDC
y0	0 ± 0
A1	1,55301 ± 0,07545
t1	5,47858 ± 0,11483
Reduced Chi-Sqr	0,37694
R-Square(COD)	0,9903
Adj. R-Square	0,98956

Fig.5: Area of the luminescence band obtained for BDC as a function of the time delay from the exciting laser pulse. The result of the fit of the data with a single exponential decay with characteristic time of $\tau_{BDC} = 5.5$ ns is also shown.

The luminescence spectra acquired for MIL-53(Al) for delay times of 5 ns and 19 ns from the laser pulse are reported in Fig. 6 (a) and (b), respectively. A more complex and interesting scenario is found compared to the simple case of BDC in molecular form. The spectra are asymmetric and exhibit a variable shape as a function of the time delay. These findings indicate that the luminescence observed in MIL-53(Al) may arise from the partial overlap of several bands with different spectroscopic properties and lifetimes. To isolate these contributions, a mathematical deconvolution of the experimental spectra in separate bands was performed. In a first attempt we have tried with only two components, but this approach led to the result that one of the band shifts towards higher energy and the FWHM of both the components bands undergo significant changes as a function of the delay time. Since these results do not have physical meaning, we have considered a deconvolution procedure involving three components' bands. This latter approach was found to give very reliable results, as discussed in detail in the following.

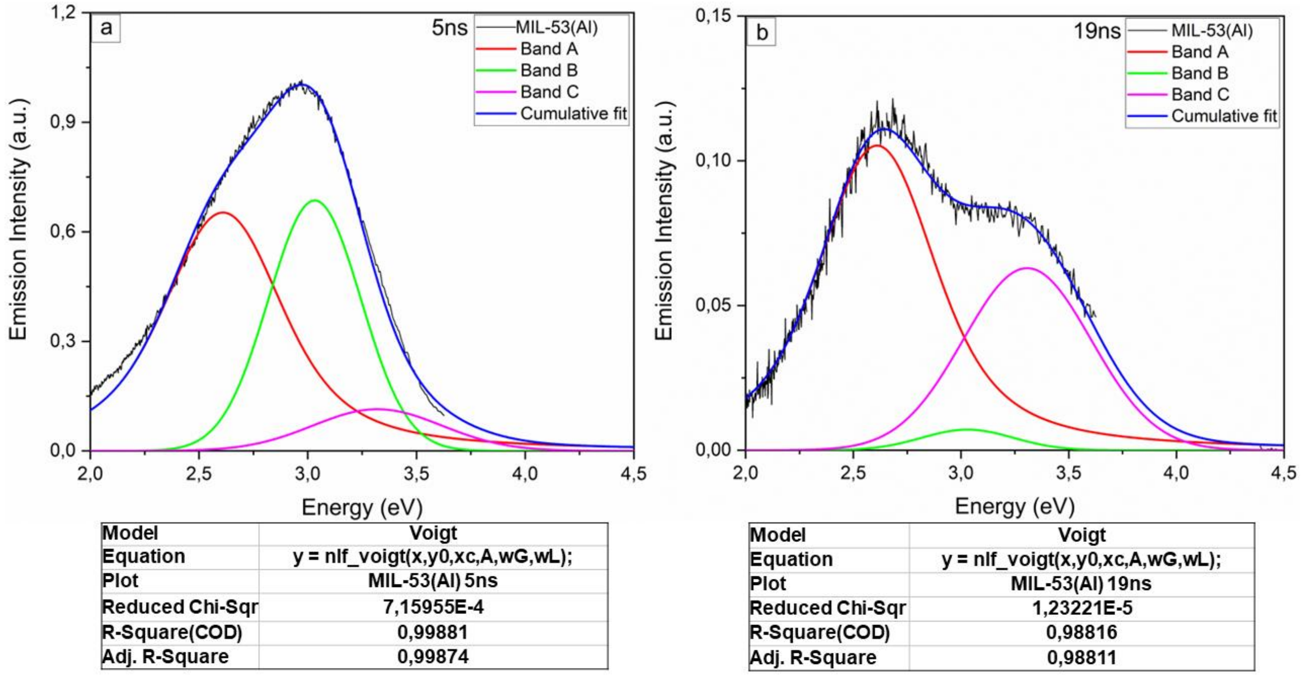

Model	Voigt
Equation	y = nlf_voigt(x,y0,xc,A,wG,wL);
Plot	MIL-53(Al) 5ns
Reduced Chi-Sqr	7,15955E-4
R-Square(COD)	0,99881
Adj. R-Square	0,99874

Model	Voigt
Equation	y = nlf_voigt(x,y0,xc,A,wG,wL);
Plot	MIL-53(Al) 19ns
Reduced Chi-Sqr	1,23221E-5
R-Square(COD)	0,98816
Adj. R-Square	0,98811

Fig. 6: MIL-53(Al) luminescence spectra obtained for delay times of (a) 5 ns and (b) 19 ns from laser pulse.

The three component bands obtained from the deconvolution procedure by using Voightian profiles were found to peak at 2.62 ± 0.05 eV, 3.02 ± 0.05 eV and 3.30 ± 0.05 eV, with FWHM of 0.66 ± 0.03 eV, 0.51 ± 0.04 eV and 0.70 ± 0.03 eV, respectively. In the following, these bands will be simply referred to as A, B and C, respectively. Upon comparing the spectra shown in Figure 6(a) and (b), it is evident that the luminescence spectrum of MIL-53(Al) mainly consists of A and B bands when measured within a few nanoseconds after the laser excitation, whereas the C band becomes noticeable after longer delay times. Peak position and FWHM of the three bands were found to be stable within the experimental uncertainty as a function of the delay time (Fig. S4).

The study of the time response of the components A, B and C pertaining to MIL-53(Al) are reported in Fig. 7(a), (b) and (c), respectively, where the area of the bands are reported as a function of the time delay from the exciting laser pulse. By assuming a single exponential decay, it was possible to fit the experimental data and to obtain an estimation of the characteristic lifetimes. The results of the fits are superimposed to the experimental data in Fig. 7, for comparison, whereas the estimated lifetimes are collected in Table 1. The values of A(0) are also reported and represent the area of the bands extrapolated at zero time delay.

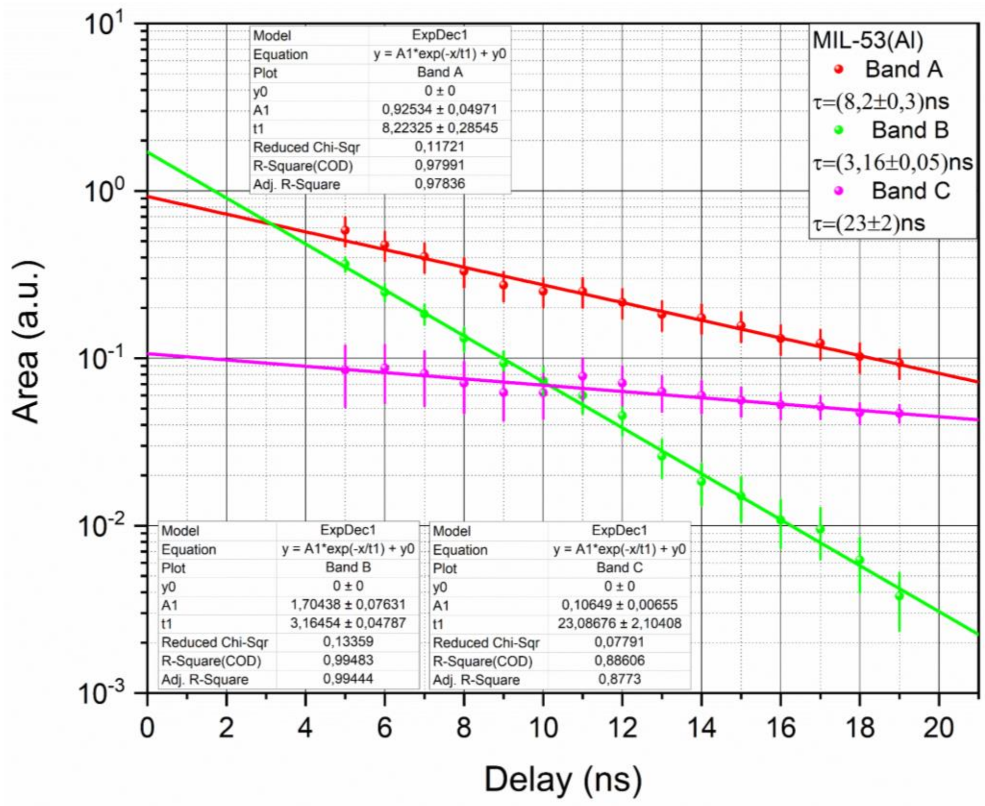

Fig. 7: Area of the luminescence bands A(a), B(b) and C(c) obtained for MIL-53(Al) as a function of the time delay from the exciting laser pulse. The results of the fit to the data with single exponential decays are also shown.

Band name	A	B	C
A(0)	0.93±0.05	1.70±0.08	0.107±0.007
τ(ns)	8.2±0.6	3.2±0.5	23±2

Table 1: Area of the photoluminescence bands extrapolated at zero time delay (A(0)) and Luminescence lifetimes (τ) obtained by fitting the emission decay curves for MIL-53(Al) with single exponential curves

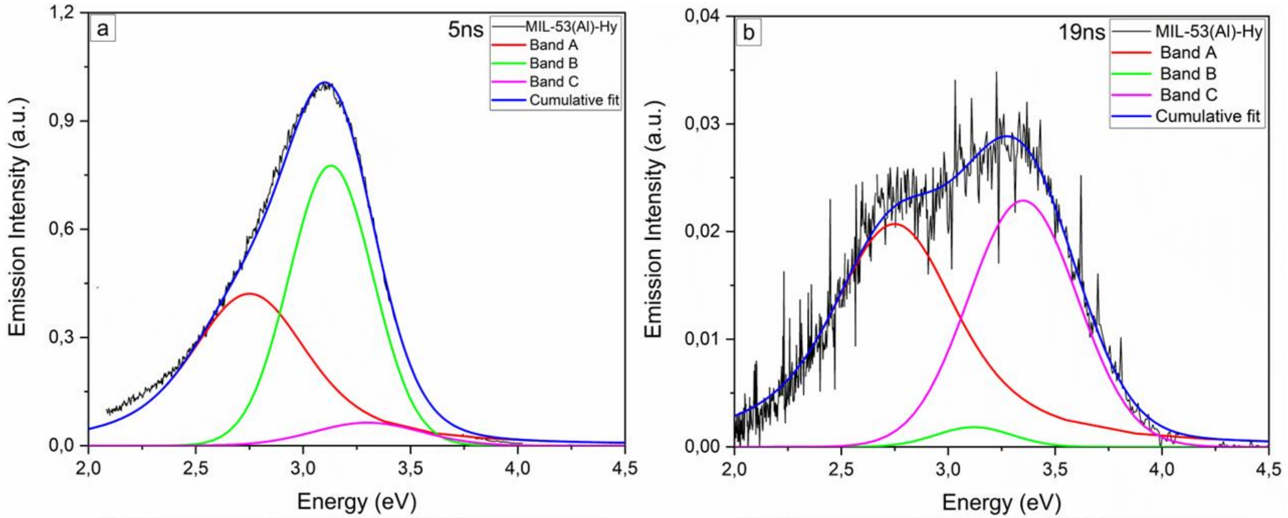

Model	Voigt
Equation	y = nlf_voigt(x,y0,xc,A,wG,wL);
Plot	MIL-53(Al)-Hy 5ns
Reduced Chi-Sqr	0,00167
R-Square(COD)	0,98342
Adj. R-Square	0,98345

Model	Voigt
Equation	y = nlf_voigt(x,y0,xc,A,wG,wL);
Plot	MIL-53(Al)-Hy 19ns
Reduced Chi-Sqr	4,67355E-6
R-Square(COD)	0,95224
Adj. R-Square	0,95232

Fig. 8: Solid state luminescence spectra acquired after a time delay of 5ns (a) and 19 ns(b) for the sample MIL-53(Al)-Hy.

Luminescence spectra obtained for MIL-53(Al)-Hy after time delays of 5 ns and 19 ns from the exciting laser pulse are reported in Fig. 8. Similar to MIL-53(Al), complex spectra are observed. By applying a three-component deconvolution of the spectra, they can be easily described by three bands spectroscopically comparable with those previously determined for MIL-53(Al). This result can be recognized by comparison of the data reported in Fig. S4 and S5, where we report peak position and FWHM of the three bands obtained for MIL-53(Al) and MIL-53(Al)-Hy, respectively. Consequently, hereafter we will assume that the bands A, B and C are representative of the main luminescence processes that can take place in the material MIL-53(Al), whereas their relative amplitudes depend on the structure and/or on the hydration state of the material.

The area of the bands extrapolated at zero time delay (A(0)) and the luminescence lifetimes (τ), obtained for MIL-53(Al)-Hy by using the same approach discussed above for MIL-53(Al), are reported in Table 2.

Band name	A	B	C
A(0)	1.3±0.1	2.0±0.2	0.113±0.005
τ(ns)	4.8±0.5	2.30±0.5	13.5±0.9

Table 2: Luminescence lifetimes (τ) and area of the bands extrapolated at zero time delay (A(0)) obtained by fitting the emission decay curves for MIL-53(Al)-Hy

4. Discussion

The deconvolution approach used in this work clearly shows the presence of three sub-bands in both MIL-53(Al) and MIL-53(Al)-Hy, denoted by A, B and C. From the careful analysis of the luminescence data presented in previous section, a strong analogy is found between the band B observed in the spectra of MOF samples and the one pertaining to BDC in molecular form. In fact these bands are peaked at 3.11 ± 0.07 eV and have FWHM 0.52 ± 0.08 eV. This result indicates a common luminescence mechanism and strongly support the attribution of the band B to a process in which both the excitation of electrons by photons and the resulting radiative decay occurs within the organic linker, also known as intra-ligand photoluminescence. The lifetime of the band B is shorter, 3.2 ± 0.5 ns, than that pertaining to the BDC molecular form, 5.5 ± 0.5 ns. This finding indicates that the former system has additional active channels for non-radiative decays with respect to the latter, which is in line with expectations considering that the linker interacts with the crystal framework. This band is not expected to be significantly influenced by the local crystalline structure of the MOF, as it is primarily localized on the linker. In line with this expectation, we have found that the relative area attributed to this band relative to the overall luminescence spectrum, evaluated just after the exciting laser pulse, is comparable in MIL-53(Al) and MIL-53(Al)-Hy, despite their quite different structures (see PXRD spectra in Fig. 1 and the related comments). This result can be evaluated qualitatively by comparing the spectra shown in Figs. 6 and 8 and quantitatively by examining the data reported in Table 3, where the percentage area of the three bands evaluated at 0 delay time with respect to the overall luminescence spectrum are reported. As shown, the percentage area of the band B is poorly affected by changing the structure of MIL-53(Al) (78%/62% = 1.2), whereas those of the other two bands, A and C, are both lower in the hydrated framework (20%/34% = 0.6 and 1.3%/3.9% = 0.3, respectively). Since the fixed excitation wavelength used for time resolved photoluminescence measurements was found to maximize all the components of the luminescence spectrum, a similar excitation process was assumed for A and C bands with respect to the B component, but a different luminescence pathway. Basing on the mechanisms proposed in previous works focused on MIL-53(Al) [30,31] and on the general optical properties of MOFs [1,2], we suggest that both A and C bands involve a ligand-to-metal charge transfer. This assumption is also in line with the reduction of the relative area of these bands observed upon hydration of MIL-53(Al), as it is well known that the presence of guest molecules into the cavities tends to obstacle the electron charge transfer process [1,43]. Since MIL-53(Al) is a breathing MOF, it is reasonable to assume that A and C bands may arises from the same electronic transition but taking place in different local crystalline structures. To further investigate this idea, in Fig. 9 the values of the area obtained just after the laser pulse for A and C bands normalized with respect to that of the B band are reported for MIL-53(Al) and MIL-53(Al)-Hy. The normalization process is necessary to eliminate the inherent experimental uncertainty affecting the absolute values of the luminescence areas, that is essentially related to the practical impossibility to obtain exactly the optical geometry every time we put a sample within the spectrometer. We selected the band B as reference because it is essentially structural-independent, as discussed above. By inspection of the data reported in Fig. 9, it evident that in both the MOF samples the relative contribution of the band A is significantly larger than that of the band C. Furthermore, it systematically increases going from hydrated sample to the activated one. These experimental findings suggest that band A is related to a transition occurring in a site involving local OP structure. Indeed, OP is most present in MIL-53(Al) than in MIL-53(Al)-Hy and prevails in both samples with respect to CP and Hy-NP, as evidenced by the PXRD spectra reported in Fig. 1 and the accompanying remarks.

Band name	A	B	C
MIL-53(Al)	34±4 %	62±6 %	3.9±05 %
MIL-53(Al)-Hy	20±4 %	78±10 %	1.3±0.2 %

Table 3: Percentage area of A, B and C bands with respect to the overall luminescence spectrum estimated at 0 delay time for MIL-53(Al) samples.

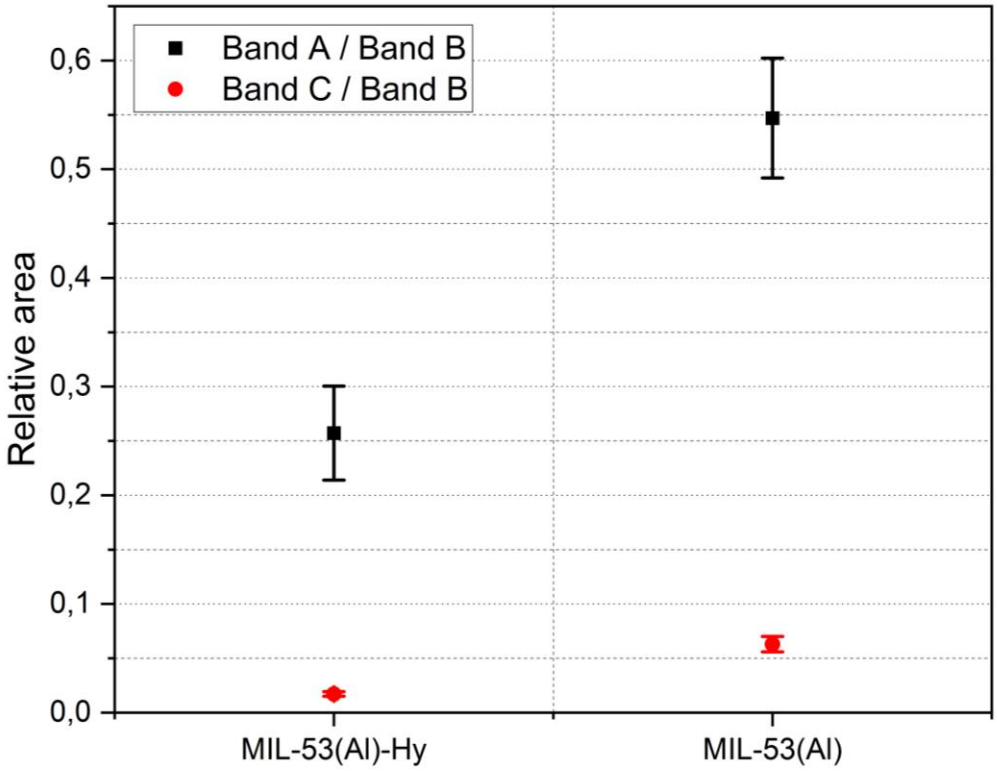

Fig. 9: Values of the area obtained just after the laser pulse for A and C bands normalized with respect to that of the B band obtained for MIL-53(Al) and MIL-53(Al)-Hy.

The last band, C, is consequently assigned to a LMCT process taking place in a site involving a closed type structure, CP or Hy-NP. Our results indicate that the luminescence bands associated to these two structures cannot be distinguished spectroscopically. This is not surprising, considering that they pertain to the same electronic transition occurring in very similar local structures. However, it is expected that the presence of the water molecule into the cavities should affect the dynamics of the decay process, potentially decreasing the transition's lifetime and quantum yield by introducing additional non-radiative channels for radiative decay. This effect is, in fact, observed and recognizable by comparing the lifetimes reported in Tables 1 and 2 for MIL-53(Al) and MIL-53(Al)-Hy, respectively. The lifetime of the C band is the double for the former sample than for the latter. Similar considerations apply to the area of the band, that is related to the quantum yield, of course, as shown in Fig. 9.

Finally, we would like to note that the attributions we suggest for the A, B and C bands also clarify the origin of the effects observed under high-power laser excitations shown in Fig. S2. These results indicate that upon high-power laser irradiation, the area of the band A increases relative to those of the other two bands, suggesting the formation of new OP structures into the material. Assuming that laser-induced heating caused water molecules to partially desorb, it is reasonable to expect that some of the cavities of the Hy-NP structure could open up.

5. Conclusions

In summary, here we report a comprehensive experimental investigation focused on the optical properties of the breathing MOF MIL-53(Al) mainly performed by ns-scale time-resolved photoluminescence measurements. Our results point out that luminescence spectra of MIL-53(Al) in powder form excited with a wavelength of 305 nm involves three distinct partially superimposed contributions, denoted by A, B and C bands, whose spectroscopic properties and lifetimes have been fully characterized. In addition, by comparing the optical and structural properties of activated- and hydrated-MIL-53(Al) samples as well as those of BDC in molecular form, we have fully unveiled the photophysics of these bands, proving for the first time that in MIL-53(Al) both intra-ligand and ligand-to-metal charge transfer luminescence transitions take place. Furthermore, we have established a connection between luminescence properties and material structure of MIL-53(Al). In fact, we have found that, while the intra-ligand process is essentially structure independent, the LMCT is structure-sensitive, allowing to distinguish between open-pore, closed-pore and hydrated narrow-pore structures. Taking into account all these results, the band A is attributed to a structure-independent intra-ligand transition, the band B to a LMCT in a site with OP structure, whereas band C to a LMCT in sites with CP or Hy-NP structures, that are distinguishable basing on their lifetimes.

Conflicts of interest

There are no conflicts to declare.

Acknowledgments

RE and REM gratefully acknowledge financial support by the European Research Council grant ADOR (Advanced Grant 787073), the EPSRC Light Element Analysis Facility Grant (EP/T019298/1) and the EPSRC Strategic Equipment Resource Grant (EP/R023751/1).

6. Reference

---

[1] M. D. Allendorf, C. A. Bauer, R. K. Bhakta and R. J. T. Houk, Chem. Soc. Rev. 38 (2009) 1330-1352. https://doi.org/10.1039/B802352M

[2] Y. Cui, Y. Yue, G. Qian and B. Chen, Chem. Rev., 112 (2) (2012), 1126-1162. https://doi.org/10.1021/cr200101d

[3] H. C. Zhou, J. R. Long and O. M. Yaghi, Chem. Rev. 112 (2) (2012) 673-674. https://doi.org/10.1021/cr300014x

[4] G. Li, H. Sun, H. Xu, X. Guo and Di Wu, J. Phys Chem. C 121 (47) (2017) 26141-26154. https://doi.org/10.1021/acs.jpcc.7b07450

[5] D. Alezi, Y. Belmabkhout, M. Suyetin, P. M. Bhatt, Ł. J. Weseliński, V. Solovyeva, K. Adil, I. Spanopoulos, P. N. Trikalitis, A.H. Emwas and M. Eddaoudi, J. Am. Chem. Soc. 137 (41) (2015) 13308-13318. https://doi.org/10.1021/jacs.5b07053

---

[6] D. Wu, X. Guo, H. Sun and A. Navrotsky, J. Phy Chem. Lett. 6 (13) (2015) 2439-2443. https://doi.org/10.1021/acs.jpclett.5b00893

[7] N. Wang, A. Mundstock, Y. Liu, A. Huang and J. Caro, Chem. Eng. Sci. 124 (2015) 27-36. https://doi.org/10.1016/j.ces.2014.10.037

[8] R. Lin, L. Ge, S. Liu, V. Rudolph and Z. Zhu, ACS Appl. Mater. Interfaces 7 (27) (2015) 14750-14757. https://doi.org/10.1021/acsami.5b02680

[9] A. Crake, K. C. Christoforidis, A. Kafizas, S. Zafeiratos and C. Petit, Appl. Catal. B 210 (2017) 131-140. https://doi.org/10.1016/j.apcatb.2017.03.039

[10] C.Yang, X. You, J. Cheng, H. Zheng and Y. Chen, Appl. Catal. B, 200 (2017) 673-680. https://doi.org/10.1016/j.apcatb.2016.07.057

[11] Y.Sun, L. Zheng, Y. Yang, X. Qian, T. Fu, X. Li, Z. Yang, H. Yan, C. Cui and W. Tan, Nano-Micro Lett. 12 (2020) 103. https://doi.org/10.1007/s40820-020-00423-3

[12] X. Chen, R. Tong, Z. Shi, B. Yang, H. Liu, S. Ding, X. Wang, Q. Lei, J. Wu and W. Fang, ACS Appl. Mater. Interfaces 10 (3) (2018) 2328-2337. https://doi.org/10.1021/acsami.7b16522

[13] S.M. Moosavi, A. Nandy, K.M. Jablonka, D. Onigari, J. P. Janet, P. G. Boyd, Y. Lee, B. Smit and H. J. Kulik, *Nat. Commun.* 11 (2020) 4068. https://doi.org/10.1038/s41467-020-17755-8

[14] F. Millange and R. I. Walton, Isr. J. Chem. 58 (2018) 1019-1035. https://doi.org/10.1002/ijch.201800084

[15] S. Tomar and V.K. Singh, Mater. Today: Proc. 43 (5) (2021) 3291-3296. https://doi.org/10.1016/j.matpr.2021.02.179

[16] F. Millange, C. Serre and G. Férey, Chem. Comm. 8 (2002) 822-823. https://doi.org/10.1039/B201381A

[17] G. Férey, Chem. Soc. Rev. 37 (2008) 191-214. https://doi.org/10.1039/B618320B

[18] I. Nevjestić, H. Depauw, K. Leus, G. Rampelberg, C. A. Murray, C. Detavernier, P. Van Der Voort, F. Callens and H. Vrielinck, J. Phys. Chem. C 120 (31) (2016) 17400-17407. https://doi.org/10.1021/acs.jpcc.6b04402

[19] E. Y. Mertsoy, X. Zhang, C. B. Cockreham, V. G. Goncharov, X. Guo, J. Wang, N. Wei, H. Sun and D. Wu, J. Phys. Chem. C 125 (25) (2021) 14039-14047. https://doi.org/10.1021/acs.jpcc.1c02623

[20] J. García-Ben, J. López-Beceiro, R. Artiaga, J. Salgado-Beceiro, I. Delgado-Ferreiro, Y. V. Kolen'ko, S. Castro-García, M. A. Señarís-Rodríguez, M. Sánchez-Andújar and J. M. Bermúdez-García, Chem. Mater. 34 (7) (2022) 3323-3332. https://doi.org/10.1021/acs.chemmater.2c00137

[21] I. Nevjestic, H. Depauw, P. Gast, P. Tack, D. Deduytsche, K. Leus, M. Van Landeghem, E. Goovaerts, L. Vincze, C. Detavernier, P. Van Der Voort, F. Callens and H. Vrielinck, Phys. Chem. Chem. Phys. 19 (2017) 24545-24554. https://doi.org/10.1039/C7CP04760F

[22] T. K. Trung, P. Trens, Philippe, N. Tanchoux, S. Bourrelly, P. L. Llewellyn, S. Loera-Serna, Sandra, C. Serre, T. Loiseau, F. Fajula and G. & Férey, J. Am. Chem. Soc. 130 (2008) 16926-16932. https://doi.org/10.1021/ja8039579

[23] T. Loiseau, C. Serre, C. Huguenard, G. Fink, F. Taulelle, M. Henry, T. Bataille, and G Férey, Chem. Eur. J. 10 (2004) 1373-1382. https://doi.org/10.1002/chem.200305413

[24] L. Chen, J. P. S. Mowat, D. Fairen-Jimenez, C. A. Morrison, S. P. Thompson, P. A. Wright and T. Düren, J. Am. Chem. Soc. 135 (42) (2013) 15763-15773. https://doi.org/10.1021/ja403453g

[25] Y. Liu, J. H. Her, A. Dailly, A. J. Ramirez-Cuesta, D. A. Neumann, C. M. Brown, J. Am. Chem. Soc. 130 (35) (2008) 11813-11818. https://doi.org/10.1021/ja803669w

---

[26] M. Mendt, B. Jee, N. Stock, T. Ahnfeldt, M. Hartmann, D. Himsl, A. Pöppl, J. Phys. Chem. C, 114 (45) (2010) 19443-19451. https://doi.org/10.1021/jp107487g

[27] A. E. J. Hoffman, L. Vanduyfhuys, I. Nevjestić, J. Wieme, S. M. J. Rogge, H. Depauw, P. Van Der Voort, H. Vrielinck, V. Van Speybroeck, J. Phys Chem. C 122 (5) (2018) 2734-2746. https://doi.org/10.1021/acs.jpcc.7b11031

[28] Y. Jiao, Z. Li, Y. Ma, G. Zhou, S. Wang and G. Lu, AIP Adv. 7 (2017) 085009. https://doi.org/10.1063/1.4999914

[29] I. Nevjestić, H. Depauw, K. Leus, V. Kalendra, I. Caretti, G. Jeschke, S. Van Doorslaer, F. Callens, P. Van Der Voort and H. Vrielinck, ChemPhysChem 16 (14) (2015) 2968-2973. https://doi.org/10.1002/cphc.201500522

[30] C.-X. Yang, H.-B. Ren and X. P. Yan, Anal. Chem. 85 (15) (2013) 7441-7446. https://doi.org/10.1021/ac401387z

[31] Y. An, H. Li, Y. Liu, B. Huang, Q. Sun, Y. Dai, X. Qin and X. Zhang, J. Solid State Chem. 233 (2016) 194-198. https://doi.org/10.1016/j.jssc.2015.10.037

[32] J. Xiao, Y. Wu, M. Li, B.-Y. Liu, X.-C. Huang and D. Li, Chem. Eur. J.19 (6) (2013) 1891-1895. https://doi.org/10.1002/chem.201203515

[33] J. Yao, Y.-W. Zhao and X.-M. Zhang, ACS Omega 3 (5) 2018 5754-5760. https://doi.org/10.1021/acsomega.8b00199

[34] Z. Wang, C.-Y. Zhu, Z.-W. Wei, Y.-N. Fan and M. Pan, Chem. Mater. 32 (2) (2020) 841-848. https://doi.org/10.1021/acs.chemmater.9b04440

[35] J. Rouquerol, P. Llewellyn and F. Rouquerol, in P. L. Llewellyn, F. Rodriquez-Reinoso, J. Rouqerol and N. Seaton (Eds.), Characterization of Porous Solids VII, Elsevier, 2007, vol. 160, pp. 49–56.

[36] P. G. Yot, Z. Boudene, J. Macia, D. Granier, L. Vanduyfhuys, T. Verstraelen, V. Van Speybroeck, T. Devic, C. Serre, G. Férey, N. Stock and G. Maurin, Chem. Comm. 50 (2014) 9462-9464. https://doi.org/10.1039/C4CC03853C

[37] G. Ortiz, G. Chaplais, J.-L. Paillaud, H. Nouali, J. Patarin, J. Raya and Claire Marichal, J. Phys. Chem. C, 118 (38) (2014) 22021-22029. https://doi.org/10.1021/jp505893s

[38] D. V. Patil, P. B. Somayajulu Rallapalli, G, P. Dangi, R. J. Tayade, R. S. Somani and H. C. Bajaj, Ind. Eng. Chem. Res. 50 (18) (2011) 10516-10524. https://doi.org/10.1021/ie200429f

[39] J. Möllmer, M. Lange, A. Moeller, C. Patzschke, K. Stein, D. Lässig, J. Lincke, R. Gläser, H. Krautscheid and R Staudt, J. Mater. Chem. 22 (2012) 10274-10286. https://doi.org/10.1039/C2JM15734A

[40] N. Heymans, S. Vaesen and G. De Weireld, Microporous and Mesoporous Mater. 154 (2012) 93-99. https://doi.org/10.1016/j.micromeso.2011.10.020

[41] A. Laybourn, K. Juliano, R. S. Ferrari-John, C. G. Morris, S. Yang, Sihai, O. Udoudo, T. L. Easun, C. Dodds, N. R. Champness, S. W. Kingman, M. Schröder, J. Mater. Chem. A 5 (2017) 7333-7338. https://doi.org/10.1039/C7TA01493G

[42] A. Pereira, A. F.P. Ferreira, A. Rodrigues, A. M. Ribeiro, M. J. Regufe, Microporous and Mesoporous Mater. 331 (2022) 111648. https://doi.org/10.1016/j.micromeso.2021.111648

[43] Y.-Q. Huang, B. Ding, S. Bin, H.-B. Song, B, Zhao, P. Ren, P. Cheng, H.-G. Wang, D.-Z. Liao and S.-P. Yan, *Chem. Comm.* 47 (2006) 4906-4908. https://doi.org/10.1039/B610185B